Ultrasonics Sonochemistry 76 (2021) 105632

Contents lists available at ScienceDirect

Ultrasonics Sonochemistry

journal homepage: www.elsevier.com/locate/ultson

Impact of solid particles on cavitation behaviors and laser-induced degradation in aqueous suspension

Chunhui Luo, Jiayang Gu, Xinchao Xu, Pingchuan Ma, Hongfeng Zhang, Xudong Ren *

Jiangsu University, No. 301 Xuefu Road, Zhenjiang, Jiangsu 212013, People's Republic of China

ARTICLE INFO

Keywords:
Laser-induced cavitation
Degradation
Rhodamine B
Sand suspension
High speed imaging

ABSTRACT

A method for degrading organic pollutants in suspension by applying laser-induced cavitation is presented. Cavitation bubbles are produced remotely by laser beams, achieving a purpose of non-contact degradation. In this work, laser-induced bubble dynamics in SiO_2 sand suspension were studied by high-speed imaging. Pulsating characteristics of cavitaiton bubbles in the infinite domain and near a solid boundary were investigated among various laser energies and sand concentrations. Furthermore, the extent of degradation after processing in suspension and the mechanism were analyzed. Results indicate that solid particles in the liquid medium reduce the extent of degradation. However, the extent of degradation may rebound at a proper sand concentration. In addition, compared to several small bubbles in a bubble string (in the infinite domain), a single larger bubble (near a solid boundary) has a much higher degradation ability.

1. Introduction

Organic water pollution has always existed with the development of industry and scientific research, common in printing and dyeing wastewater or laboratory wastage [1–3]. Traditional physical, chemical and biological degradation methods [4–6] have certain limitations such as demanding a large space to place the equipment, may lead in secondary pollution, etc. As a result, hydraulic and ultrasonic cavitation degradation methods have been proposed in recent years. Laser-induced cavitation bubbles pulsate after generated in the water, and the radicals produced by laser ablation and cavitation behaviors during the pulsating period are capable of decomposing the organic dye [7–9]. Saxena [10] investigated the degradation of tannery waste effluent using hybrid hydrodynamic cavitation. Patil et al. [11] using ultrasound cavitation to degradate thiamethoxam together with intensifying additives. However, limitations exist when using hydrodynamic or ultrasound cavitation, such as complex device and poor controllability [12].

Cavitation was first discovered as a destructive phenomenon, while cavitation erosion may cause huge erosion damage on hydraulic equipment [13–15]. As a result, interdisciplinary studies are demanded due to the complexity of the cavitation erosion origin [16]. Laser technology together with hydraulic cavitation is one of the combinations to further study the dynamics of the cavitation bubbles. Laser-induced cavitation can generate single bubbles or bubble strings near the focus points of the laser beams. As a result, studies on pulsation behaviors and mechanism may be carried out more easily to explain the phenomenon of cavitation. Brujan and Nguyen [17,18] investigated the effects of a boundary on double bubbles induced by laser beams. Yang and Orthaber [19,20] studied the functions of various solid materials during the pulsating period of cavitation bubbles. Most of the present researches on cavitation degradation are focused on hydraulic and ultrasonic cavitation degradation methods, while few are using laser cavitation (LC) technology. Gu et al. [21] first proposed a novel method of laser cavitation (LC) degradation, and studied the influence of laser and medium parameters on the degradation efficiency of LC degradation method.

Suspension is a common liquid medium in the process of degradation. On the one hand, untreated sewage contains particles, on the other hand, particles may be intentionally added in the liquid, such as solid catalysts. In the study of degradation, cavitation is often combined with other degradation methods to improve the degradation efficiency [22]. In these cases, catalyst particles may be introduced into the medium. These particles not only promote the degradation, but also impact the pulsating behaviors of cavitation bubbles. As a result, studying the effect of particles in suspension on cavitation degradation is necessary. However, present researches on cavitation are relatively limited to clear water conditions, only a few experiments on cavitation dynamics have been conducted in sand suspension environment [23], and research on cavitation degradation in suspension is rear.

* Corresponding author.
E-mail address: renxd@mail.ujs.edu.cn (X. Ren).

https://doi.org/10.1016/j.ultsonch.2021.105632
Received 17 March 2021; Received in revised form 9 June 2021; Accepted 12 June 2021
Available online 18 June 2021

This work focused on investigating the dynamics of laser-induced bubbles and the effect of laser cavitation degradation in sand suspension environment. SiO_2 powder was selected as non-catalyst particles so that the effect of particles on cavitation degradation can be studied independently. A high-speed camera was used to observe and measure the features of the single bubbles or bubble strings in sand suspension. Pulsating characteristics of cavitation bubbles in infinite domain and near a solid boundary were investigated, and the degradation mechanism were analyzed on the basis of the results.

2. Experimental procedures

2.1. Experimental setup

As shown in Fig. 1, 1064 nm wavelength laser beams from the generator (Q-switched Nd: YAG) were focused above a bottom block (1060 aluminum alloy). SiO2 powder was added in the solution and suspended by hand stirring with a glass bar. It seemed that the particles would go to sink at the cell bottom in about 30 s after stopping the stirring, while the camera work may be completed within the first 3 s. The diameters of the powder particles were nearly 50 μm. In this work, water tanks and test tubes were selected as liquid containers. A transparent water tank was considered as an ideal container for taking photographs, resulting from the flat profiles of the tank. However, the cross section of the water tank is relatively large, and the depth of the solution in the tank is not enough when the amount of the liquid is small. A certain depth of the solution in the container was necessary when laser beams were focused below the liquid surface. As a result, test tubes were used as an alternative of water tanks in the degradation experiments.

2.2. Reagent and analysis

Reagent: Rhodamine B (RhB, C28H31N2O3Cl) used in this work was analytical reagent grade, and the suspension was diluted to 20 mg/L by tap water as a initial concentration.

Analysis: Concentration of RhB in the solution was analyzed using UV spectrophotometer (Cary 8454 UV–Vis, Agilent). The wavelength was set to 554 nm. The concentration of unknown sample was calculated based on the standard calibration curve, according to the absorbance of known samples. Repeated experiments were performed at least five times. Mean value and standard deviation were calculated to check the reproducibility of results.

3. Results and discussion

3.1. Degradation experiments and mechanism

In this section, experiments of laser cavitation degradation of RhB in SiO_2 suspension were carried out. The diameter of particles was 50 μm, the degradation time was 60 min, and the pulse frequency of the laser generator was set to 2 Hz.

Fig. 2 (a) shows the degradation of RhB suspension with sand concentration near a solid boundary. It can be observed that the degradation decreases with sand concentration in total. However, the degradation rebounds at a sand concentration of 0.04%. Fig. 2 (b) shows the relationship between the degradation of RhB suspension and sand concentration in the infinite domain. The tendency of the curves is similar to those near a solid boundary. The degradation rebounds at a sand concentration of 0.06%. When the sand concentration reaches 0.07%, the extent of degradation under the laser energy of 100 mJ is almost 0% and even negative. RhB molecules can not be oxidized in this case and the negative value results from the evaporation effect. The position of the peak on the horizontal axis (0.04% in Fig. 2 (a), 0.06% in Fig. 2 (b), and 0.025% in Fig. 6 (c-d)) depends on the sedimentation of the suspension particles and the stirring effect.

Fig. 2 (c) shows the degradation of RhB suspension with laser energy near a solid boundary. It can be observed that the degradation increases with the laser energy. When the laser energy is 250 mJ, the degradation of RhB reached 93.21% in the water and 86.9% in the suspension, respectively. Fig. 2 (d) shows the relationship between the degradation of RhB suspension and laser energy in the infinite domain. The degradation increases with the laser energy. When the laser energy is 250 mJ, the degradation of RhB reached 25.21% in the water and 18.50% in the suspension, respectively. The trend of the degradation rate gets gradual when the laser energy exceed 200 mJ. At beginning of the expansion period, the plasma provides initial energy for the pulsation. When the energy increases to a certain extent, the plasma absorption limit the cavitation behaviors.

The degradation kinetics at various sand concentrations were investigated in Fig. 3 (a). The relationship between the concentration of RhB (C) and the degradation time (t) can be expressed by the following equation [21]:

$$Ln\left(\frac{C}{C_0}\right) = kt \tag{1}$$

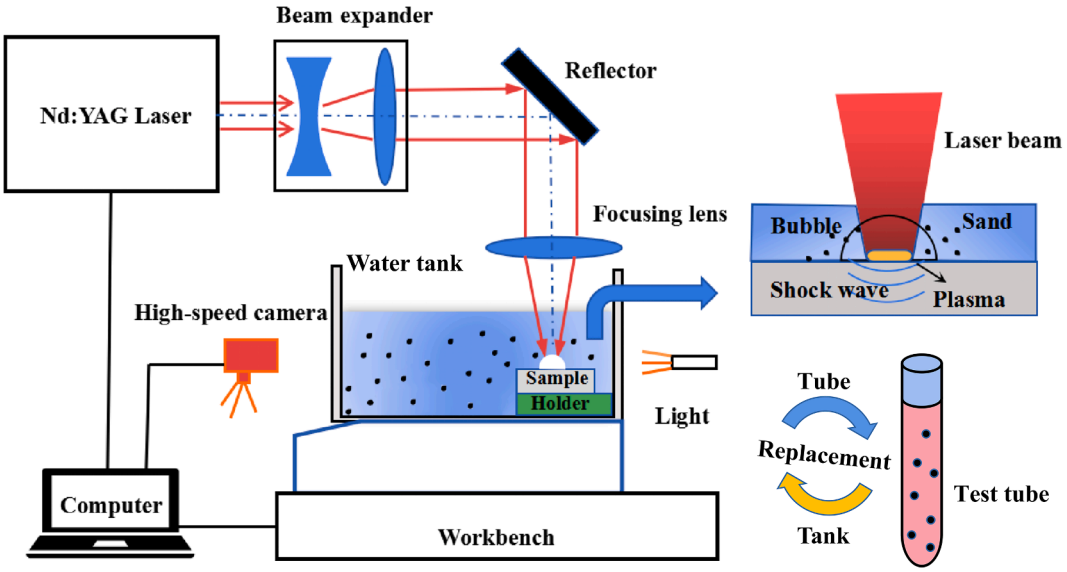

Fig. 1. Schematic diagram of experimental setup.

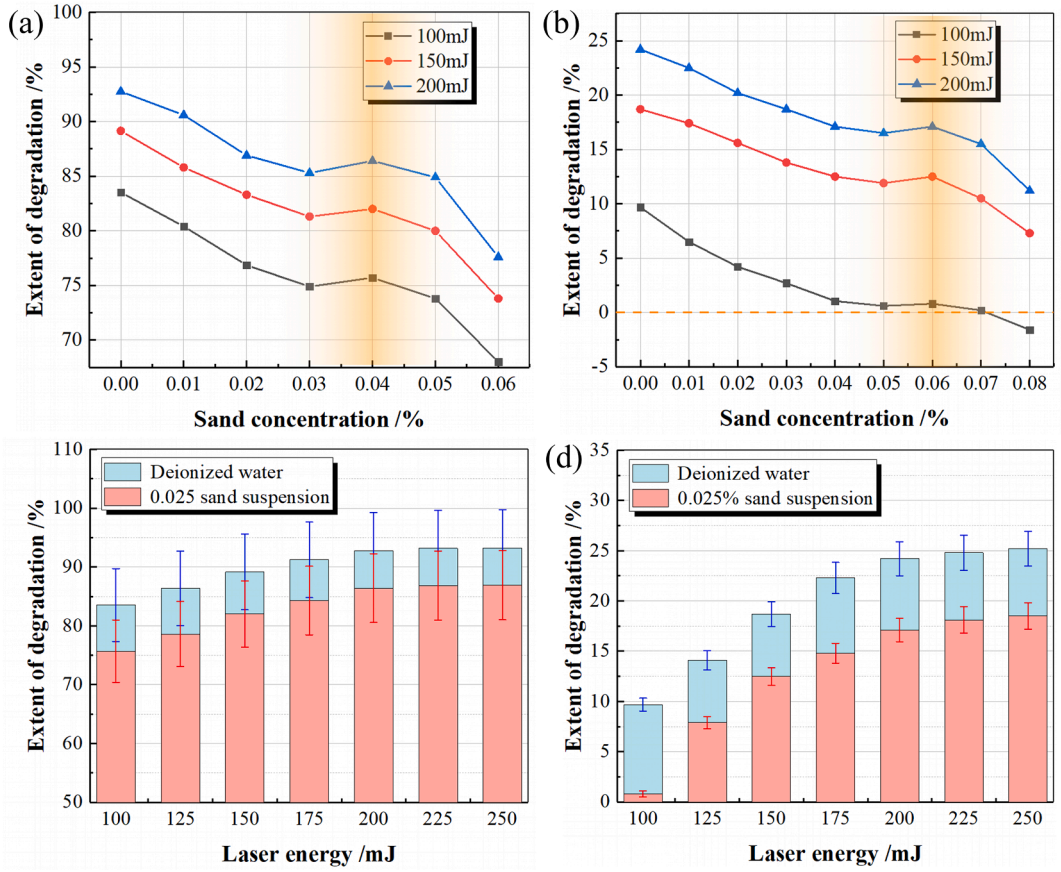

Fig. 2. Extent of degradation (a) under different sand concentration near a solid boundary, (b) under different sand concentration in the infinite domain, (a) under different laser energy near a solid boundary, (b) under different laser energy in the infinite domain.

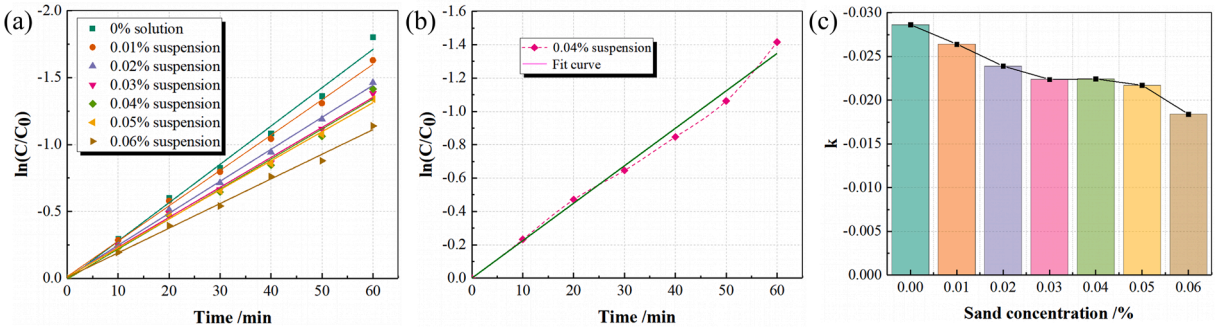

Fig. 3. (a) Fit curve of ln(C/C0) with processing time under various sand concentrations, (b) A single fit curve when the sand concentration is 0.04%, (c) The value of k in Equation (1) under different sand concentrations.

where C_0 is the initial concentration, and k is a constant.

In Fig. 3 (a), a fit curve of RhB concentration ratio ($\ln(C/C_0)$) is obtained according to Equation (1). In logarithmic coordinates, the ratio of RhB concentration decreases as linear, indicating that pseudo-first-order kinetic is applicable in this case. Fig. 3 (b) shows one of the curves (0.04% suspension) in Fig. 3 (a). The laser beams were focused on the solid boundary, resulting in the partial shedding of the material. As a result, the suspension environment was effected, and the scatter points deviated from the straight line after 40 min. Fig. 3 (c) shows the curve and the value of k in Equation (1), and the trend of the curve is similar to which in Fig. 2 (a).

Fig. 4 (a) shows the evolution of a laser-induced shock wave and a laser-induced bubble near a solid boundary. A shock wave (SW_0) is generated and begin to expand due to the initial pressure near the focused point. The expansion velocity decays in liquid before the distance passed by shock wave reaches the radius of the spot (SW_1). Afterwards, the shock wave expands in a spherical shape (SW_2) and the expansion velocity of which decays faster [24,25]. The water near the focused point is heated and pushes away the surrounding water, resulting in the expansion of cavitation bubbles. Fig. 4 (b) shows the mechanism and stirring action of LC degradation method. When the plasma bursts in water near the focused point, free radicals (·OH and ·H) are produced from H_2O molecules, and the first shock wave is generated. When the cavitation bubble collapses after several pulsation, the free radicals and second shock wave is generated [21]. The shock waves push and disperse the particles along the direction of the radiation, promoting the stirring action. If the laser beam is focused near the boundary, a water jet may be produced to lash the solid surface, depending on the

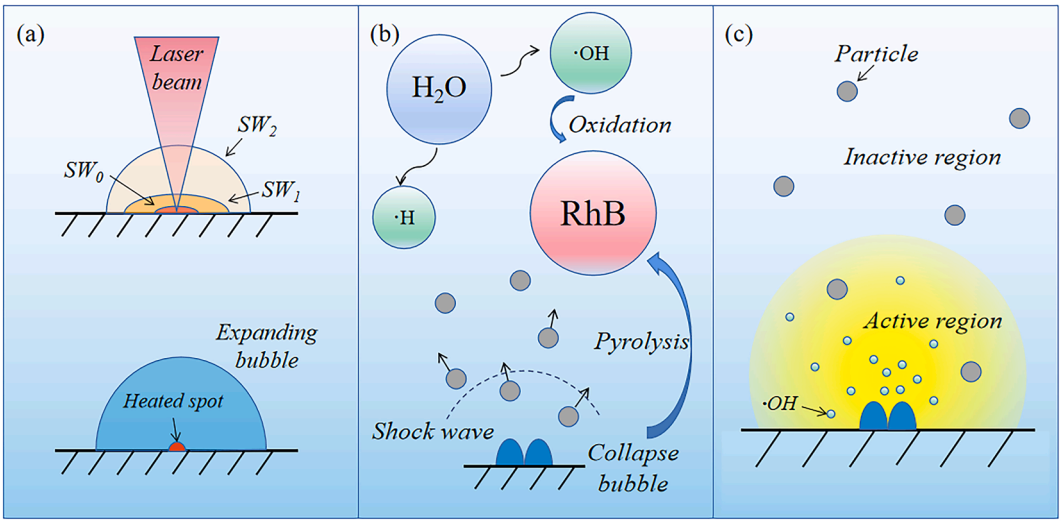

Fig. 4. Diagrammatic sketch of (a) evolution of a laser-induced shock wave and a laser-induced bubble, (b) stirring action and RhB degradation by LC, (c) degradation area in the container.

value of parameter γ (The ratio of stand-off distance H to maximum bubble radius R). The oxidation of ·OH radicals is the main factor to impel the degradation of RhB. In addition, the RhB molecules are thermally decomposed before the cavitation behaviors due to the energy of the laser beam. When the bubble collapses, localized extreme environments can also result in the thermal decomposition of RhB molecules. In Fig. 4 (c), differing from other degradation methods, LC can only deal with the compounds in the local area, while RhB far away from the focused point may not be degraded.

3.2. Impact of sand particles on cavitation behaviors and degradation extent

As shown in Fig. 5, cavitation behaviors were studied for further

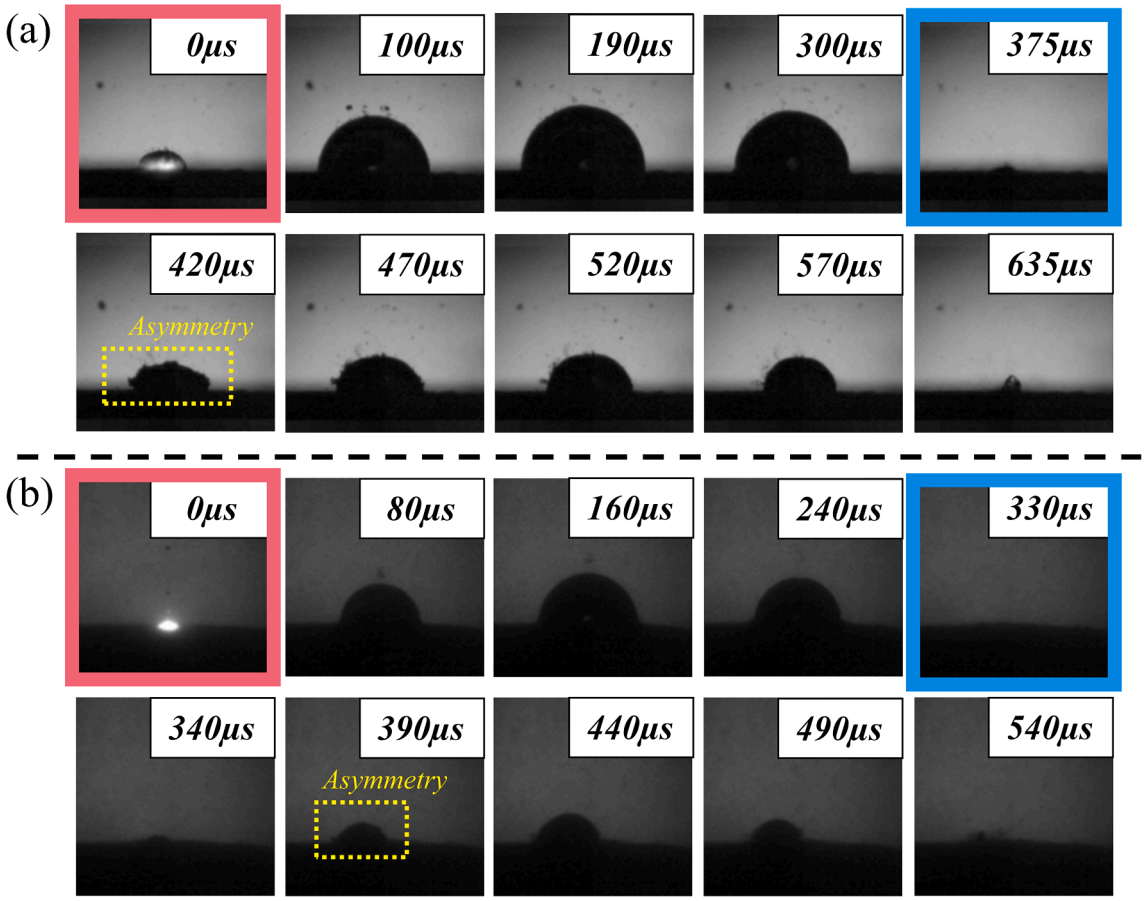

Fig. 5. The sequence graph of the cavitation bubble near a solid boundary when the laser energy is 100 mJ (the original resolution ratio of each photo is 128*128 pixel) (a) in the tap water, (b) in 0.025% sand suspension.

investigating the mechanism of particles impact on the degradation extent. In Fig. 5 (a), when a laser beam is focused on the surface of the material through the liquid medium to produce high-temperature plasma (t = 0 μs). The large energy density exceeds the breakdown threshold to form a strong light. After absorbing the energy of the plasma, the pressure inside the bubble gets stronger than that of the external liquid medium [26]. As a result, the bubble expand and push the surrounding liquid to flow radially. The expansion velocity of the bubble is relatively fast at first (t = 0–100 μs), resulting from the large pressure difference between two sides of the bubble wall. Subsequently, the bubble continues to expand outwards until reaching the maximum radius. After the bubble reaching its maximum radius, the internal pressure of the bubble gets smaller than the pressure outside the bubbles. As a result, the bubble begins to shrink inwards until the bubble reaches the minimum radius. The pressure discrepancy and the inertia of the bubble wall lead to the multiple pulsations of the bubble. At end of the first shrinkage period, the bubbles shrink to a very small radius. The pressure inside the bubbles is very high, resulting in a strong shock wave to the liquid [27,28]. When t is from 375 μs to 635 μs, the bubble is in the expansion period of the second pulsation period, and the maximum radius of which is much smaller than that in the first pulsation period, resulting from acoustic radiation and energy dissipated by the liquid. Cavitation bubbles show regular hemispheres during the first pulsation. However, the shapes of the bubbles become irregular during the second pulsation, especially in the initial stage of the expansion (t = 420 μs). This phenomenon is similar to which studied by Nguyen [18]. The shock wave released after the first pulsation period causes the bubble in the second pulsation period to deviate from the regular hemispherical shape [29].

Fig. 5 (b) shows a sequence diagram of bubbles near a solid boundary in suspension with a laser energy of 100 mJ and a sand concentration of 0.025%. The expansion and shrinkage of the bubbles near a solid boundary in suspension are also due to the pressure difference at both sides of the bubble walls. Under a same energy, the maximum bubble diameter and the pulsation period in the water are larger than those in suspension. This phenomenon indicates that part of the laser energy is transferred as internal and kinetic energy of the sand particles.

Fig. 6 shows the curves of bubbles' pulsating features with sand concentration under different laser energy near a solid boundary in suspension. In Fig. 6 (a), Cavitation bubbles are treated as regular hemispheres, and the vertical length is considered as the radius of the bubbles.

Fig. 6 (c) shows the relationship between the sand concentration and the bubble radius. The value of the bubble radius decreases with sand concentration under the same laser energies. When the sand concentration increases to 0.025%, the maximum bubble radius rebound and produce a peak. Fig. 6 (d) show the curves of the maximum bubble volume. The change trend is consistent with the change of the pulsation period in Fig. 6 (c). The changing amplitude of the maximum volume is larger than that of the maximum radius, resulting from the calculation formula of sphere volume. The pulsation of the bubbles are weakened due to the add of the sand particles. Particles absorb part of the laser energy, however, more nuclei is led into the water. As a result, cavitation may be promoted within a certain sand concentration range.

In addition in Fig. 6 (b), the maximum radius of the bubble increases with the laser energy. However, the increase rate of the bubble radius is different in various ranges of laser energy. The maximum bubble radius increases rapidly and then is retarded, resulting from the plasma absorption effect.

Fig. 7 shows the mechanism of bubble pulsation in suspension and the mechanism of LC degradation method. In the suspension, particles may produce more gas nuclei, and affect the generation and

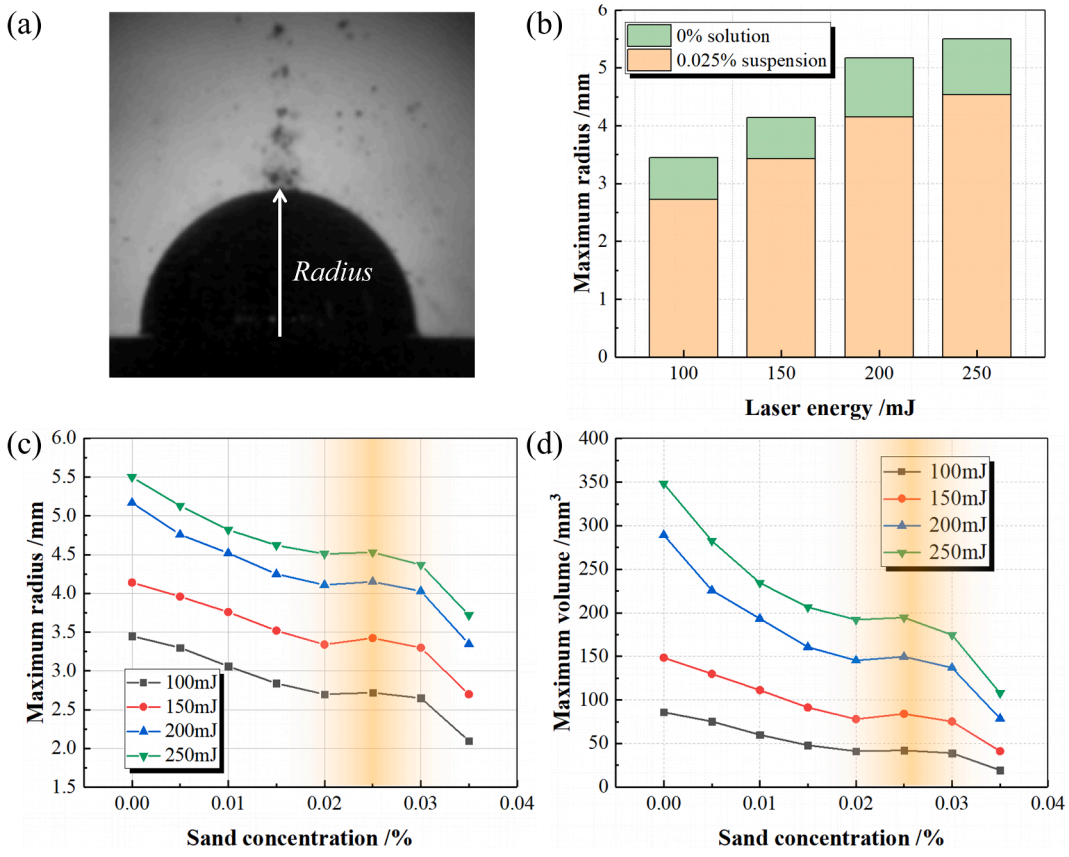

Fig. 6. (a) Measurement method of the bubble near a soild boundary, (b) the relationship between laser energy and maximum radius, (c) curves of maximum radius under different sand concentrations, (d) curves of maximum volume under different sand concentrations.

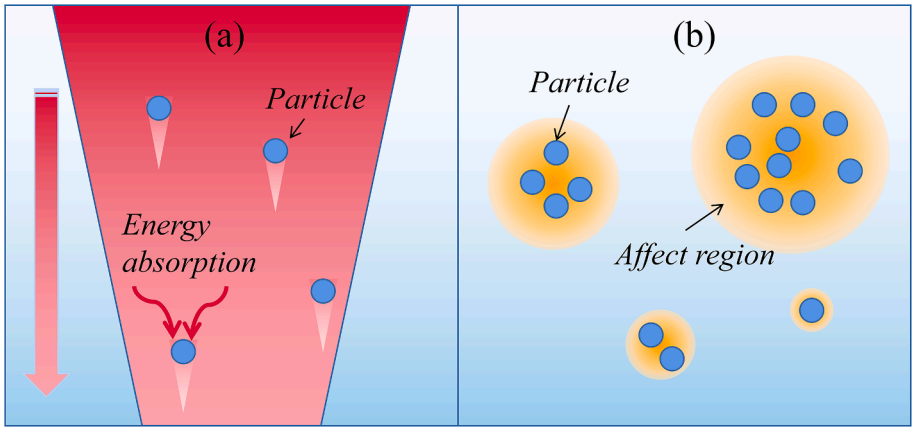

Fig. 7. (a) Negative effects of particles on cavitation behaviors, (b) Positive effects of particles on cavitation behaviors.

development of cavitation bubbles [30–31]. However, excessive particle concentration in suspension may directly affect and destroy the liquid environment where cavitation occurs. A appropriate concentration of particles may improve the effect of hydraulic cavitation [32]. Compared with other cavitation methods, laser-induced cavitation has an additional feature. Due to the limitation of the optical path, the laser beam can only generate laser cavitation through a fixed optical path. Particles along the optical path may affect the propagation of laser beams, resulting in a smaller initial expansion velocity, as shown in Fig. 7 (a).

Sufficiently large particles may provide more nuclei and affect the macroscopic properties of the liquid (viscosity, etc.) [31]. According to the theory of Sutherland [33], when the particle diameter is larger than 2 μm, the possibility of collision will be greatly increased. Su's [31] study takes 10–100 μm as the value of particle diameter to investigate the interaction between particle size and ultrasonic cavitation erosion. The diameters of the sand particles in this study are about 50 μm, which is a appropriate value to affect the cavitation behaviors. The sand particles can only collide with bubbles in this area. Bubble pulsation may be enhanced at a proper concentration, as shown in Fig. 7 (b). However, as the concentration of sand particles increases, the probability of collision between the bubbles and sand particles also increases. As a result, the probability of sand collision increases and the bubble pulsation is weakened. It can be concluded that solid particles with proper concentration can promote laser cavitation and cause a rebound in the descent curve [34].

Fig. 8 (a) shows the dynamic snapshots of cavitation bubbles in the water, and the laser energy is set to 100 mJ. Bubble strings are generated when the laser energy exceeds the breakdown threshold of the liquid, and the pulsating features of the largest bubbles in the strings were recorded in this study. The expansion and shrinkage processes of the largest bubble last for about 80 μs each. From the pulsation pattern of the bubble string, a trend can be observed that several close small bubbles may eventually mix into a small amount of larger bubbles.

Fig. 8 (b) shows the pulsation sequence diagram in sand suspension with a laser energy of 100 mJ and a sand concentration of 0.025%. The number, size and pulsation period of the bubbles in suspension get reduced, compared to the cavitation bubbles in the water. Particles absorb part of the laser energy, impeding the formation of the bubbles.

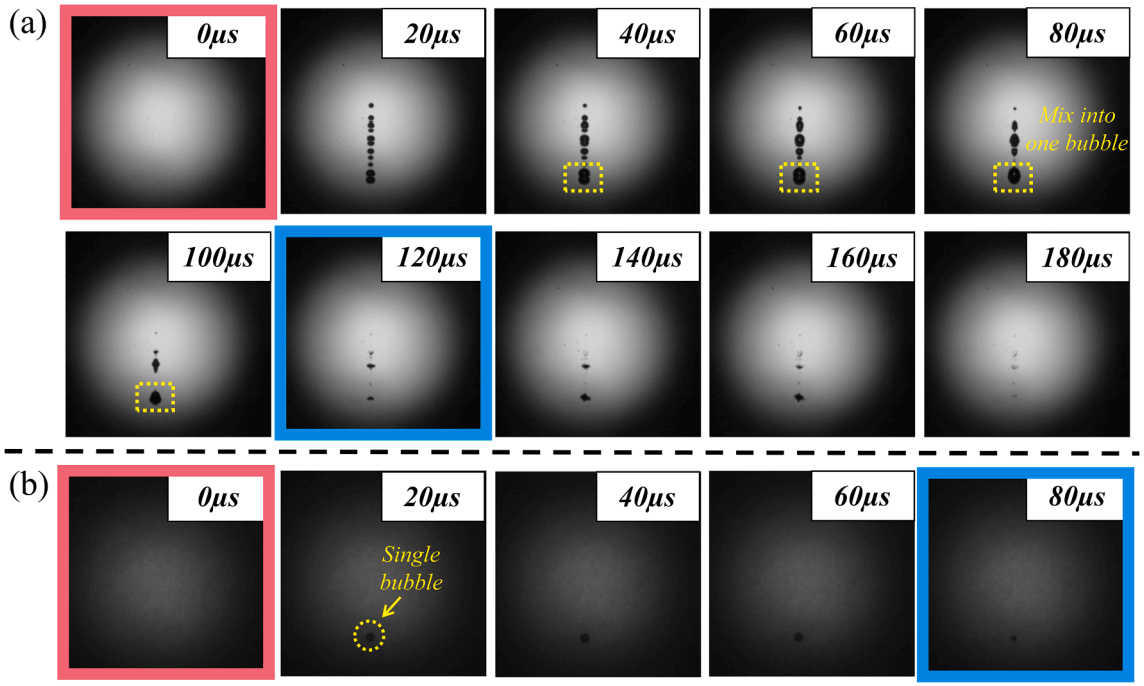

Fig. 8. The sequence graph of the cavitation bubble in the water when the laser energy is 100 mJ (the original resolution ratio of each photo is 256*256 pixel) (a) in the tap water, (b) in 0.025% sand suspension.

In addition, single bubbles were observed in Fig. 8 (b). Single laser-induced bubbles are generated more easily in deionized water, or in the case of small laser energy. However in this study, a larger sand concentration consumes the laser energy, making it difficult to produce bubble strings in the non-focus area, or can only produce very small bubbles. As a result, single bubbles can be observed.

Fig. 9 (a) shows the curves of bubbles' pulsating features with sand concentration under different laser energy in the infinite domain in suspension. A bubble string contains several bubbles after generated in the infinite domain and the bubbles in the string may not keep regularly spherical, resulting from the intensive compression between the bubbles. As a result, the outline of the bubble string was sketched and the volume was calculated according to the body of revolution.

In Fig. 9 (c-d), the maximum bubble diameter in the water is much larger than that in suspension. When the sand concentration is 0.025%, the maximum diameter of the bubbles is slightly larger than that in 0.02% suspension. As the sand concentration continues to increase to 0.03%, the maximum diameter of the bubbles decreases. The changing amplitude of the maximum volume is larger than that of the maximum radius (especially in the the water), resulting from the bubble number in a string.

Fig. 9 (b) shows the relationship between the number of bubbles and the concentration of sand particles under different laser energy in infinite domain of the suspension. Considering that discrepancy of the pulsation period may exist among the bubbles in a string, the value of the bubble number is measured when the largest bubble expands to the maximum diameter. The tendency of the bubble number under a laser energy of 150 mJ is similar to that of the bubble diameter in Fig. 9 (c). When the laser energy is 100 mJ, the number of the bubbles in the string decreases to 0.8 (sand concentration is 0.025%), and finally the value turns to 0 (sand concentration is 0.03%). The values under the laser energy of 100 mJ are too small to form the regular curve. When the laser energy is 200 mJ, the center distances between the adjacent bubbles in the string are too small. The bubbles squeeze with together and achieve a relatively stable structure, resulting in a gradual curve.

Fig. 10 (a-b) shows the relationship between the maximum volume of bubbles and the extent of degradation when the bubbles/strings are generated near a solid boundary or in the infinite domain, separately. The volume of the bubble string is the sum of all the bubbles in the string. The degradation extent increases with the maximum volume of the cavitation bubbles. This phenomenon is applicable to the bubbles generated in different areas (near a solid boundary or in the infinite domain). Differences exist between the bubbles near a solid boundary and in the infinite domain. The degradation extent near a solid boundary is much larger than that in the infinite domain, resulting from the bubble shape, the pulsating forms and the bubble volume. The volume of the bubble near a solid boundary (19.39–289.27 mm^3) is much larger than the total volume of the bubbles in the infinite domain (0–15.10 mm^3), which is the major factor of the differences.

Cavitation pulsation is a process of continuous energy dissipation, while each pulsation may dissipate a portion of energy until the bubble finally collapses. In order to explore the potential energy of the cavitation bubble during the pulsation process, a specific equation is quoted [35]:

$$E_{Bi} = \frac{4}{3}\pi p_{\infty} R_{max}^3 \quad (2)$$

Where: is the static pressure in the liquid, and R_{max} is the maximum radius of the bubble.

The values of degradation extent indicate that a single larger bubble near a solid boundary has a much higher degradation ability than several small bubbles in a bubble string in the infinite domain. The total volume of bubbles in a string is smaller than a single bubble, resulting in the disparity of bubble energy, according to Equation (2).

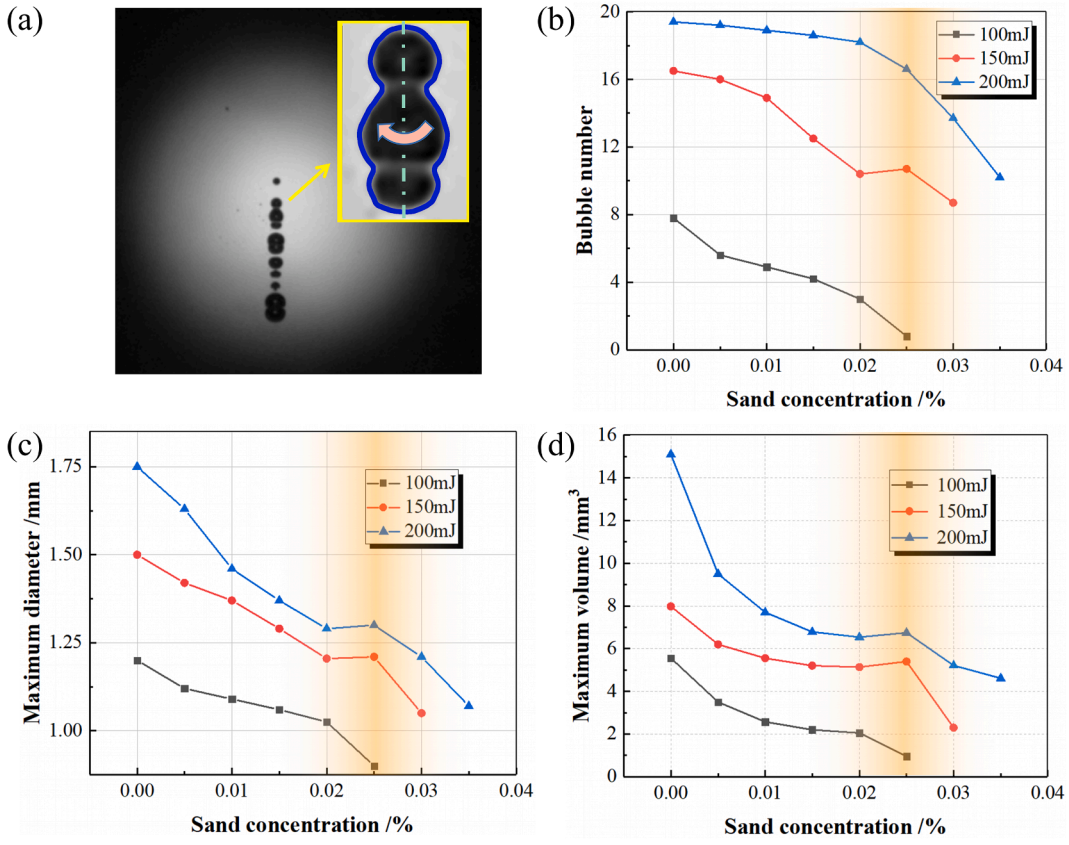

Fig. 9. (a) Measurement method of the bubble in the infinite domain, (b) the relationship between bubble numbers and sand concentration, (c) curves of maximum radius under different sand concentrations, (d) curves of maximum volume under different sand concentrations.

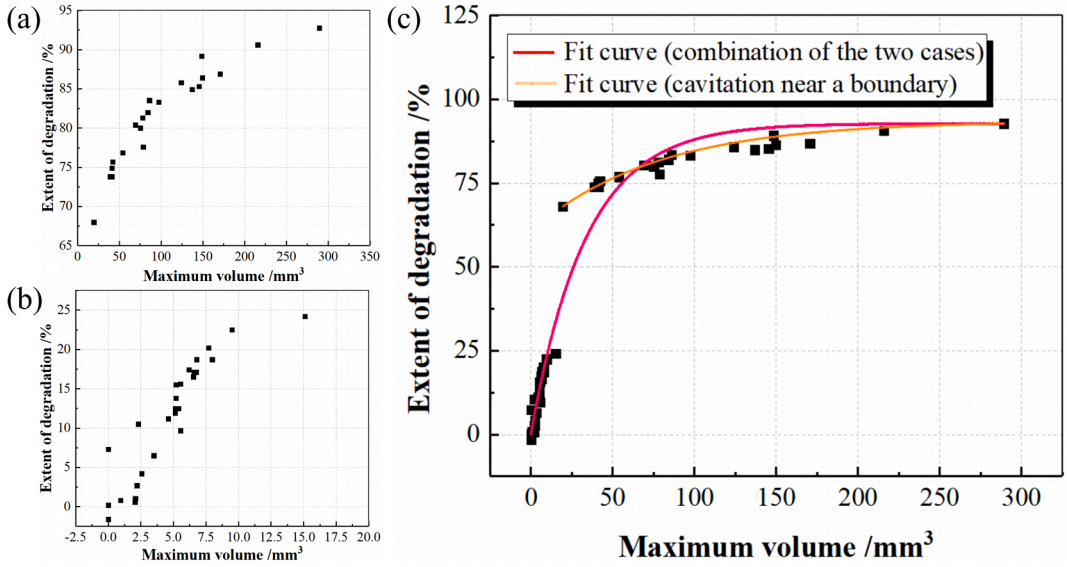

Fig. 10. The relationship between the maximum volume of bubbles and the extent of degradation (a) near a solid boundary, (b) in the infinite domain, (c) the combination of the two cases, together with the fit curve.

In Fig. 10 (c), the global fit curve (combination of the two cases) indicates that the extent of degradation increases fast when the maximum bubble volume is small, and then get retarded as the maximum bubble volume increases. The bubble shape and the pulsating forms are also the influencing factors of the degradation extent. As a result, the global fit curve and the fit curve near a boundary are not completely consistent. Only qualitatively results can be observed from the fit curve, especially when the volume is similar in the two cases (15.10 mm^3 in the infinite domain and 19.39 mm^3 near a boundary).

Most of the final degradation extent in recent research is between 60 and 100%, and some of the advanced methods have higher degradation extent (more than 90%) [36–38]. The optimal degradation extent in this work is 93.21%. Qualitatively, laser-induced degradation method has unique advantages and limitations.

Laser-induced degradation method can degrade the solution remotely and non-contact, which is safer and can reduce the influence of the solution on the devices. In addition, the modular design of laser-based unit system is easier to realize in industrial application. However, as a relatively new research, this study only degrades small amount of solution. Further research and optimization are needed to increase the industrial application value.

4. Conclusion

In this paper, high-speed imaging is used to study the dynamics of laser-induced cavitation bubbles and the effects of laser cavitation (LC) degradation method. Various laser energies and sand concentrations were selected to investigate the pulsation characteristics of cavitaiton bubbles in the infinite domain (bubble strings) and near a solid boundary (single bubbles). The results show that when the laser energy exceeds the liquid breakdown threshold, a spherical bubble string will be formed in infinite domain, and a hemispherical bubble will be formed near the boundary. The intensity of bubble pulsation (size, pulsating period and number of the bubbles) and extent of degradation have similar trend. The extent of degradation is promoted by a larger laser energy. However, the values tend to balance due to the plasma absorption when the laser energy exceeds a certain value. Particles in the liquid medium reduce the extent of degradation. However, the extent of degradation may rebound at a proper sand concentration. The rebound peak is located at a sand concentration of 0.025% in the ideal case, while higher concentrations are required in practice. Compared to several small bubbles in a bubble string (in the infinite domain), a single larger bubble (near a solid boundary) has a much higher degradation ability.

CRediT authorship contribution statement

Chunhui Luo: Conceptualization, Investigation, Writing - original draft. **Jiayang Gu:** Methodology, Writing - review & editing. **Xinchao Xu:** Methodology. **Pingchuan Ma:** Writing - review & editing. **Hongfeng Zhang:** Writing - review & editing. **Xudong Ren:** Writing - review & editing.

Declaration of Competing Interest

The authors declare that they have no known competing financial interests or personal relationships that could have appeared to influence the work reported in this paper.

Acknowledgments

The authors are grateful to the projects supported by the National Natural Science Foundation of China (Grant No. 51975261), Innovation Team of Six Talents Peaks in Jiangsu Province (Grant No.2019TD-KTHY-005).

References

[1] M. Xie, H.K. Shon, S.R. Gray, M. Elimelech, Membrane-based processes for wastewater nutrient recovery: technology, challenges, and future direction, Water Res. 89 (2016) 210–221, https://doi.org/10.1016/j.watres.2015.11.045.
[2] D. Tan, B. Bai, D. Jiang, L. Shi, S. Cheng, D. Tao, S. Ji, Rhodamine B induces long nucleoplasmic bridges and other nuclear anomalies in Allium cepa root tip cells, Environ. Sci. Pollut. Res. 21 (5) (2014) 3363–3370, https://doi.org/10.1007/s11356-013-2282-9.
[3] R. Saravanan, E. Sacari, F. Gracia, M.M. Khan, E. Mosquera, V.K. Gupta, Conducting PANI stimulated ZnO system for visible light photocatalytic degradation of coloured dyes, J. Mol. Liq. 221 (2016) 1029–1033, https://doi.org/10.1016/j.molliq.2016.06.074.
[4] A. Akbari, J.C. Remigy, P. Aptel, Treatment of textile dye effluent using a polyamide-based nanofiltration membrane, Chem. Eng. Process 41 (7) (2002) 601–609, https://doi.org/10.1016/S0255-2701(01)00181-7.
[5] P.K. Malik, Dye removal from wastewater using activated carbon developed from sawdust: adsorption equilibrium and kinetics, J. Hazard. Mater. 113 (1-3) (2004) 81–88, https://doi.org/10.1016/j.jhazmat.2004.05.022.
[6] H. An, Y.i. Qian, X. Gu, W.Z. Tang, Biological treatment of dye wastewaters using an anaerobic-oxic system, Chemosphere 33 (12) (1996) 2533–2542, https://doi.org/10.1016/S0045-6535(96)00349-9.

[7] L.A. Crum, Comments on the evolving field of sonochemistry by a cavitation physicist, Ultrason. Sonochem. 2 (2) (1995) S147–S152, https://doi.org/10.1016/1350-4177(95)00018-2.
[8] A. Henglein, Sonochemistry: historical developments and modern aspects, Ultrasonics 25 (1) (1987) 6–16, https://doi.org/10.1016/0041-624X(87)90003-5.
[9] X. Wang, J. Wang, P. Guo, W. Guo, G. Li, Chemical effect of swirling jet-induced cavitation: degradation of rhodamine B in aqueous solution, Ultrason. Sonochem. 15 (4) (2008) 357–363, https://doi.org/10.1016/j.ultsonch.2007.09.008.
[10] S. Saxena, V.K. Saharan, S. George, Enhanced synergistic degradation efficiency using hybrid hydrodynamic cavitation for treatment of tannery waste effluent, J Clean Prod. 198 (2018) 1406–1421, https://doi.org/10.1016/j.jclepro.2018.07.135.
[11] P.B. Patil, S. Raut-Jadhav, A.B. Pandit, Effect of intensifying additives on the degradation of thiamethoxam using ultrasound cavitation, Ultrason. Sonochem. 70 (2021) 105310, https://doi.org/10.1016/j.ultsonch.2020.105310.
[12] P.R. Gogate, G.S. Bhosale, Comparison of effectiveness of acoustic and hydrodynamic cavitation in combined treatment schemes for degradation of dye wastewaters, Chem. Eng. Process. Process Intensif. 71 (2013) 59–69, https://doi.org/10.1016/j.cep.2013.03.001.
[13] W. Deng, Y. An, G. Hou, S. Li, H. Zhou, J. Chen, Effect of substrate preheating treatment on the microstructure and ultrasonic cavitation erosion behavior of plasma-sprayed YSZ coatings, Ultrason. Sonochem. 46 (2018) 1–9, https://doi.org/10.1016/j.ultsonch.2018.04.004.
[14] I. Tzanakis, M. Hadfield, I. Henshaw, Observations of acoustically generated cavitation bubbles within typical fluids applied to a scroll expander lubrication system, Exp. Therm. Fluid Sci. 35 (8) (2011) 1544–1554, https://doi.org/10.1016/j.expthermflusci.2011.07.005.
[15] R. Singh, S.K. Tiwari, S.K. Mishra, Cavitation erosion in hydraulic turbine components and mitigation by coatings: current status and future needs, J. Mater. Eng. Perform. 21 (7) (2012) 1539–1551, https://doi.org/10.1007/s11665-011-0051-9.
[16] W.H. Xian, D.G. Li, D.R. Chen, Investigation on ultrasonic cavitation erosion of TiMo and TiNb alloys in sulfuric acid solution, Ultrason. Sonochem. 62 (2020) 104877, https://doi.org/10.1016/j.ultsonch.2019.104877.
[17] E.A. Brujan, T. Ikeda, K. Yoshinaka, Y. Matsumoto, The final stage of the collapse of a cloud of bubbles close to a rigid boundary, Ultrason. Sonochem. 18 (1) (2011) 59–64, https://doi.org/10.1016/j.ultsonch.2010.07.004.
[18] T.T.P. Nguyen, R. Tanabe, Y. Ito, Effects of an absorptive coating on the dynamics of underwater laser-induced shock process, Appl Phys A-Mater 116 (3) (2014) 1109–1117, https://doi.org/10.1007/s00339-013-8193-2.
[19] Y.X. Yang, Q.X. Wang, T.S. Keat, Dynamic features of a laser-induced cavitation bubble near a solid boundary, Ultrason. Sonochem. 20 (4) (2013) 1098–1103, https://doi.org/10.1016/j.ultsonch.2013.01.010.
[20] U. Orthaber, R. Petkovšek, J. Schille, L. Hartwig, G. Hawlina, B. Drnovšek-Olup, A. Vrečko, I. Poberaj, Effect of laser-induced cavitation bubble on a thin elastic membrane, Opt. Laser Technol. 64 (2014) 94–100, https://doi.org/10.1016/j.optlastec.2014.05.008.
[21] J. Gu, C. Luo, W. Zhou, Z. Tong, H. Zhang, P. Zhang, X. Ren, Degradation of Rhodamine B in aqueous solution by laser cavitation, Ultrason Sonochem. 68 (2020) 105181, https://doi.org/10.1016/j.ultsonch.2020.105181.
[22] A.A. Pradhan, P.R. Gogate, Degradation of p-nitrophenol using acoustic cavitation and Fenton chemistry, J. Hazard Mater. 173 (1-3) (2010) 517–522, https://doi.org/10.1016/j.jhazmat.2009.08.115.
[23] H. Jin, F. Zheng, S. Li, C. Hang, The role of sand particles on the rapid destruction of the cavitation zone of hydraulic turbines, Wear. 112 (2) (1986) 199–205, https://doi.org/10.1016/0043-1648(86)90240-1.
[24] N.A. Inogamov, V.A. Khokhlov, Y.V. Petrov, V.V. Zhakhovsky, Hydrodynamic and molecular-dynamics modeling of laser ablation in liquid: from surface melting till bubble formation, Opt Quant Electron. 52 (2) (2020), https://doi.org/10.1007/s11082-019-2168-2.
[25] N.A. Inogamov, V. Zhakhovsky, et al., Picosecond-Nanosecond Laser Flash, Formation of powerful Elastic Waves in Crystals, and Shock Peening, ISSW 32 (2019) 3077–3106, https://doi.org/10.3850/978-981-11-2730-4_506-cd.
[26] K. Nahen, A. Vogel, Plasma formation in water by picosecond and nanosecond Nd: YAG laser pulses: transmission, scattering, and reflection, Bios Europe, International Society for Optics and Photonics (1996), https://doi.org/10.1117/12.260881.
[27] Y.V. Petrov, N.A. Inogamov, et al., Condensation of laser-produced gold plasma during expansion and cooling in a water environment, Contrib Plasm Phys. 419 (2019), https://doi.org/10.1002/ctpp.201800180.
[28] Y.V. Petrov, V.A. Khokhlov, V.V. Zhakhovsky, N.A. Inogamov, Hydrodynamic phenomena induced by laser ablation of metal into liquid, Appl Surf Sci. 492 (2019) 285–297, https://doi.org/10.1016/j.apsusc.2019.05.325.
[29] A. Sasoh, K. Watanabe, Y. Sano, N. Mukai, Behavior of bubbles induced by the interaction of a laser pulse with a metal plate in water[J], Appl Phys A 80 (7) (2005) 1497–1500, https://doi.org/10.1007/s00339-004-3196-7.
[30] H. Chen, S. Liu, J. Wang, D. Chen, Study on effect of microparticle's size on cavitation erosion in solid-liquid system, J Appl Phys. 101 (10) (2007) 103510, https://doi.org/10.1063/1.2734547.
[31] K. Su, J. Wu, D. Xia, Classification of regimes determining ultrasonic cavitation erosion in solid particle suspensions, Ultrason. Sonochem. 68 (2020) 105214, https://doi.org/10.1016/j.ultsonch.2020.105214.
[32] J. Stella, R. Alcivar, Influence of addition of microsized alumina particles on material damage induced by vibratory cavitation erosion, Wear. 436-437 (2019) 203027, https://doi.org/10.1016/j.wear.2019.203027.
[33] K.L. Sutherland, Physical chemistry of flotation; kinetics of the flotation process, J Phys & Colloid Chem. 52 (1948) 394, https://doi.org/10.1021/j150458a013.
[34] T. Tuziuti, K. Yasui, M. Sivakumar, Y. Iida, N. Miyoshi, Correlation between Acoustic Cavitation Noise and Yield Enhancement of Sonochemical Reaction by Particle Addition, J Phys Chem A 109 (21) (2005) 4869–4872, https://doi.org/10.1021/jp0503516.
[35] B.-B. Li, H.-C. Zhang, J. Lu, X.-w. Ni, Experimental investigation of the effect of ambient pressure on laser-induced bubble dynamics, Opt Laser Technol 43 (8) (2011) 1499–1503, https://doi.org/10.1016/j.optlastec.2011.05.016.
[36] S. Das, A.P. Bhat, P.R. Gogate, Degradation of dyes using hydrodynamic cavitation: Process overview and cost estimation, J Water Process Eng. 42 (2021) 102126, https://doi.org/10.1016/j.jwpe.2021.102126.
[37] S. Mosleh, M.R. Rahimi, Intensification of abamectin pesticide degradation using the combination of ultrasonic cavitation and visible-light driven photocatalytic process: Synergistic effect and optimization study, Ultrason. Sonochem. 35 (2017) 449–457, https://doi.org/10.1016/j.ultsonch.2016.10.025.
[38] S. Raut-Jadhav, D.V. Pinjari, D.R. Saini, S.H. Sonawane, A.B. Pandit, Intensification of degradation of methomyl (carbamate group pesticide) by using the combination of ultrasonic cavitation and process intensifying additives, Ultrason. Sonochem. 31 (2016) 135–142, https://doi.org/10.1016/j.ultsonch.2015.12.015.